Journal of Advanced Research 30 (2021) 159–170

Contents lists available at ScienceDirect

Journal of Advanced Research

journal homepage: www.elsevier.com/locate/jare

Genomics-guided identification of a conserved CptBA-like toxin-antitoxin system in *Acinetobacter baumannii*

Shahira A. ElBanna [a], Nayera A. Moneib [a], Ramy K. Aziz [a,b,*], Reham Samir [a,b,*]

[a] Department of Microbiology and Immunology, Faculty of Pharmacy, Cairo University, 11562 Cairo, Egypt
[b] The Center for Genome and Microbiome Research, Cairo University, Cairo, Egypt

GRAPHICAL ABSTRACT

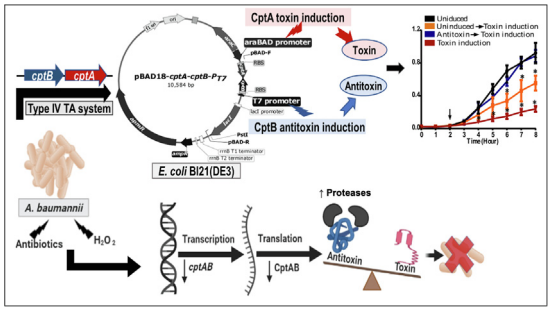

ARTICLE INFO

Article history:
Received 1 September 2020
Revised 18 November 2020
Accepted 19 November 2020
Available online 23 November 2020

Keywords:
Acinetobacter baumannii
Toxin-antitoxin
Antimicrobial resistance
Molecular biology
Plasmids
Stress factors
Bioinformatics

ABSTRACT

Introduction: Toxin-antitoxin (TA) systems are widespread among bacteria, archaea and fungi. They are classified into six types (I-VI) and have recently been proposed as novel drug targets.
Objectives: This study aimed to screen the pathogen *Acinetobacter baumannii*, known for its alarming antimicrobial resistance, for TA systems and identified a CptBA-like type IV TA, one of the least characterized systems.
Methods: In silico methods included secondary structure prediction, comparative genomics, multiple sequence alignment, and phylogenetic analysis, while *in vitro* strategies included plasmid engineering and expression of the TA system in *Escherichia coli* BL21, growth measurement, and transcription analysis with quantitative reverse-transcription polymerase chain reaction.
Results: Comparative genomics demonstrated the distribution of CptBA-like systems among Gram-negative bacteria, while phylogenetic analysis delineated two major groups, in each of which *Acinetobacter* spp. proteins clustered together. Sequence alignment indicated the conservation of *cptA* and *cptB* in 4,732 strains of *A. baumannii* in the same syntenic order. Using *A. baumannii* recombinant *cptA* and *cptB*, cloned under different promoters, confirmed their TA nature, as *cptB* expression was able to reverse growth inhibition by CptA in a dose-time dependent manner. Furthermore, transcriptional analysis of *cptBA* in clinical and standard *A. baumannii* strains demonstrated the downregulation of this system under oxidative and antibiotic stress.
Conclusion: Combining in silico and *in vitro* studies confirmed the predicted TA nature of a *cptBA*-like system in *A. baumannii*. Transcriptional analysis suggests a possible role of *cptBA* in response to antibiotics and stress factors in *A. baumannii*, making it a promising drug target.

Peer review under responsibility of Cairo University.
* Corresponding authors at: Department of Microbiology and Immunology, Faculty of Pharmacy, Cairo University, 11562 Cairo, Egypt.
E-mail addresses: ramy.aziz@pharma.cu.edu.eg (R.K. Aziz), reham.samer@pharma.cu.edu.eg (R. Samir).

https://doi.org/10.1016/j.jare.2020.11.007
2090-1232/

Introduction

Toxin-antitoxin (TA) systems are recently identified small genetic elements, composed of toxin genes and their cognate antitoxins. Toxin proteins target DNA replication, mRNA stability, protein synthesis, cell-wall biosynthesis, affecting cell division and therefore accounting for bacteriostatic or bactericidal activity. Thus, TA systems are being considered for antimicrobial therapy, especially as discovering drug targets for classic antimicrobial agents is becoming more and more difficult.

According to the nature and mode of interaction of the antitoxin, TA systems are classified into six types: I-VI [1]. All known toxins are proteins, while antitoxins are either proteins (types II, IV, and V) or non-coding RNAs (types I and III). Under normal conditions, a toxin and its cognate antitoxin are co-transcribed so that the antitoxin neutralizes the toxin. However, under unfavorable conditions, any change in the cell homeostasis will affect the labile antitoxin and hence the toxin effect predominates, leading to either growth inhibition or cell death [2].

In type IV TA system, both the toxin and antitoxin are proteins; yet, they do not interact together, as with type II TA system, but rather compete on the same target [1,3]. An example of a type IV TA system is the *yeeU/yeeV* module of *E. coli*, in which YeeU and YeeV compete on stabilizing the cytoskeletal proteins, MreB and FtsZ, which are essential for cell division [4]. *cptA/cptB* (also known as *ygfX/ygfY*) is another example of a type IV TA system, first characterized in *E. coli*, that also stabilizes MreB and FtsZ cytoskeletal proteins [5].

TA systems are either plasmid-encoded or chromosomal. Plasmid-encoded TA systems mediate postsegregational killing and thus help in plasmid stabilization among cells, specifically plasmids carrying virulence factors that are needed during host infection, as in the case of *Shigella flexneri*, *Enterococcus faecalis*, enteroinvasive *E. coli* or *Salmonella* spp. [6]. Chromosomally encoded TA systems contribute to programmed cell death in addition to other important functions, such as mediating stabilization of superintegrons that encode for resistance, virulence and metabolic proteins, such as *parA/parD*, *higA/higB*, and *phd/doc* TA modules in *Vibrio cholera* [7]. TA pairs were also reported to protect against phage infection by inducing abortive infection that help in preventing the spread of phages in the bacterial population such as *mazEF* type II TA in *E. coli* [8].

TA systems are believed to be present in most bacteria, archaea and fungi. In bacteria, fourteen TA families have been identified in different bacterial classes, including Gram-positive (e.g., *Streptococcus* and *Staphylococcus* spp.), Gram-negative (e.g., *E. coli* and *Acinetobacter* spp.), and acid-fast organisms (e.g., *Mycobacterium tuberculosis*) [1,9]. Jurenaite et al. [10] detected four functional TA loci in *Acinetobacter baumannii*, which are RelB/RelE, HigB/HigA, HicA/HicB and SplT/SplA.

A. baumannii is one of the most common causes of hospital-acquired pneumonia [11,12]. It is considered one of the pandrug-resistant bacteria [13] and is classified as an "ESKAPE" pathogen [14]. It accounts for a wide range of infections, such as wound, skin, soft tissue, urinary tract, and bloodstream infections, as well as meningitis. *A. baumannii* ventilator-associated pneumonia and bloodstream infections are those that lead to the highest mortality rates [15,16]. The severity of *A. baumannii* is attributed to its pathogenicity together with its ability to evade antibiotic treatment either by resistance or persistence mechanisms [15].

Persistence is a characteristic phenotype that bacteria only acquire under certain conditions, including antibiotic pressure, and other environmental factors, such as starvation, oxidative stress, extreme temperature, and the host immune system [3,17]. In bacterial persistence, cells enter in a dormant state upon exposure to unfavorable conditions, generating transient antibiotic tolerance in bacteria [3]. Some clinical isolates of *A. baumannii* tend to form persister cells, which transiently enter into a dormant state upon exposure to antibiotic treatment [18]. Among contributors to persistence in *A. baumannii* are TA systems [19]. Both plasmid-encoded and chromosomal TA systems affect pathogenicity through modulating bacterial growth and death under different conditions, aiming to decrease the population to limit bacterial needs under different stressors [1,9].

Here, we aimed to screen *A. baumannii*, being a public health threat, for novel TA systems, and we discovered a previously unidentified CptBA-like system, which we investigated to better understand this type IV TA system in *A. baumannii*. To this end, we constructed and used a dual-promoter expression vector to express this *A. baumannii* TA in *E. coli*, and demonstrated that CptB is toxin and CptA is its cognate antitoxin. Additionally, we studied the expression of this system in *A. baumannii* under stress.

Materials and methods

Ethical approval

All research protocols, including safety measures, storage of samples, and data confidentiality, were checked and approved by the Faculty of Pharmacy, Cairo University, Ethical committee (Approval # MI 1786, July 25, 2016). The study involved no human subjects or experimental animals, and the clinical samples used were already biobanked at Faculty of Pharmacy, Department of Microbiology and Immunology, with no attached data related to human subjects or their confidentiality.

Bacterial strains and growth conditions

Bacterial strains and plasmids used in this study are listed in Table S1 and Table 1, respectively. *A. baumannii* ATCC 17978 and *E. coli* BL21(DE3) strains were routinely cultivated in Luria-Bertani (LB) broth or on LB Agar (Difco, USA) at 37 °C. Biobanked clinical *A. baumannii* isolates (designated AB01, AB02, AB03) from

Table 1
List of plasmids used in this study.

Plasmids	Characterization	Source/ Reference
pET28b (+)	Expression vector with IPTG-inducible promoter, T7 (P_{T7}) and kanamycin resistant gene, *kanR*	Department of Microbiology plasmid collection/ Novagen, USA
pBAD18 ori	Expression vector with apramycin resistant gene, *ApmR*. Modified form of pBAD18 plasmid, with 1337 bp PCR product containing the replication origin of cryptic plasmid pWH1277 from *Acinetobacter lwoffii* DSM30013	Dr. Stephen Lory, Harvard Medical School
pBAD42	Expression vector with arabinose-inducible promoter, araBAD (P_{BAD}) and spectinomycin/streptomycin resistant gene, *spR*/*smR*	[41]
pET28b-*cptB-cptA*	Derivative of pET28b containing *cptA-cptB* where the *cptB* antitoxin gene is under the control of the P_{T7} promoter; *kanR*	This study
pBAD18-*cptA-cptB-*P_{T7}	Derivative of pBAD18 containing *cptA-cptB-*P_{T7} promoter and *lacI* gene where the *cptA* toxin gene become under the control of the arabinose pBAD promoter; *apmR*	This study
pBAD42-*cptBA*	Derivative of pBAD42 containing *cptBA* under the control of the arabinose pBAD promoter, *smR*	This study

Faculty of Pharmacy, Cairo University collection were also used for transcriptional analysis. When necessary, antibiotics were added to *E. coli* cultures at the following concentrations: kanamycin sulfate (Serva, Germany), 30 μg/ml, streptomycin sulfate (Sigma-Aldrich, Germany), 50 μg/ml, apramycin sulfate (UNIPHARMA, Egypt), 50 μg/ml. Electrocompetent *E. coli* cells were prepared and transformed with different vectors according to Woodall's protocol [20].

Screening for TA systems in A. baumannii

The Toxin-Antitoxin database (TADB, URL: https://bioinfo-mml.sjtu.edu.cn/TADB2/index.php, [21]) was used for preliminary screening of *A. baumannii* ATCC17978 genome for TA systems. Amino acid sequences of potential TA systems were retrieved from the NCBI database. Among the retrieved sequences are the *A. baumannii* ATCC 17978 CptBA-like proteins with accession numbers APP30065.1 and APP30064.1. The distribution and conservation of CptBA system-like proteins and their encoding genes among different bacteria were analyzed on the NCBI website, by the Basic Local Alignment Search Tool (BLAST) (https://blast.ncbi.nlm.nih.gov/Blast.cgi)—including BlastP (BLASTP 2.10.0+), BlastN (BLASTN 2.10.0+) and tBlastN (2.11.0) programs [22,23]. Maximum likelihood phylogenetic analysis of CptA and CptB among different bacterial spp. was conducted by MEGA version X [24]. Chromosomal context alignment was performed with the Compare Region tool in the SEED server [25].

The Constrained Consensus TOPology prediction server tool (CCTOP, http://cctop.enzim.ttk.mta.hu/) was used for predicting the CptA topology and its localization in *A. baumannii* membrane compared to the studied CptA in *E. coli*.

Transcription analysis

A. baumannii ATCC 17978 cells were grown at 37 °C, with shaking at 180 rpm, to mid-exponential growth phase (estimated by an optical density $(OD)_{600nm}$ of ~0.5). Samples were drawn, and total RNA was extracted by RNeasy Mini kit (Qiagen, Germany). cDNA was synthesized by the Promega Reverse Transcriptase Kit (Promega, USA) and subjected to quantitative polymerase chain reaction (qPCR) analysis. qPCR was performed in a Rotor-Gene-Q real-time PCR instrument (Qiagen, Malaysia), with a SensiFAST™ SYBR Lo-ROX Kit (Bioline, UK).

To determine the difference in expression of the *cptBA*-like system on *A. baumannii* standard strain or clinical isolates, we exposed the bacteria to different stresses, including high temperature (42 °C) for 30 min, oxidative stress (10 mM H_2O_2, Lona, Egypt) for 30 min, and different antibiotics, at concentrations above their minimal inhibitory concentrations, for 45 min. Antibiotics used were ciprofloxacin (at 32 μg/ml), meropenem (at 32 μg/ml), and streptomycin (at 256 μg/ml). Primers used for the quantification of the *cptA* and *cptB* genes together with housekeeping gene are listed in Table S2. The relative abundance of mRNA of each gene was expressed as fold change compared to the experiment control, determined by the ΔΔCt method [26].

Plasmid construction

Plasmids (Table 1) were constructed as follows:

■ *Construction of pET28b-cptB-cptA.*

The *cptA* and *cptB* open reading frames (ORFs) were amplified from *A. baumannii* ATCC 17978 genomic DNA. The *cptB*-F/R primer pair (Table S2) was used to amplify a genomic segment containing *cptB* with 50 bp upstream, containing the ribosome-binding site (RBS). However, *cptA* had to be amplified on two steps. First, the ORF was amplified with primers *cptA*-F/R (Table S2); then, it was fused with its 50 bp RBS, which was amplified by another primer pair (RBS-F/R, Table S2) by overlap-extension PCR and the primer pair RBS-F/*cptA*-R (Table S2). Finally, the DNA fragments of each ORF (*cptA* and *cptB*) and its corresponding RBS were digested with *Eco*RI-HF (NEB, USA), and then ligated by T4 DNA Ligase (Takara Bio, Japan) at their digested 3′end to ensure opposite orientation.

Both the *cptB-cptA* DNA fragment and the pET28b (+) plasmid were digested by *Nco*I-HF (NEB, USA) and *Sac*I (Promega, USA), then ligated together to generate pET28b-*cptB-cptA*, in which the *cptB* (antitoxin gene) would be under control of T7 promoter (P_{T7}).

■ *Construction of the dual pBAD18-cptA-cptB-P_{T7}.*

The primer pair GTApBAD-F/R (Table S2) was used to amplify the DNA fragment containing the *cptA-cptB-*P_{T7} promoter and *lacI* gene. The amplified DNA fragment was cloned in pBAD18 ori by the Gibson assembly cloning kit (NEB, USA) to generate the dual promoter plasmid, in which the *cptA* (toxin gene) is under the control of the arabinose-inducible promoter, araBAD (P_{BAD}), while the *cptB* (antitoxin gene) is under the IPTG-inducible promoter, T7 (P_{T7}). This method was adopted from Zheng, et al. [27].

■ *Construction of pBAD42-cptBA.*

A DNA fragment containing the *cptB-cptA* locus and its predicted promoter was amplified from the *A. baumannii* genomic DNA with the primer pair *cptBA*-F/R (Table S2) and cloned into the pBAD42 digested plasmid.

E. coli growth analysis

Wild-type *E. coli* BL21(DE3) was grown in LB broth, while *E. coli* BL21(DE3) harboring the selection-expression plasmid, with and without the cloned TA system genes, were grown in LB containing 50 μg/ml apramycin. Either type of cells was incubated at 37 °C with shaking overnight at 180 rpm, and their OD_{600} was adjusted to ~0.04. Culture growth was monitored either by OD_{600nm} measurement every hour (for up to 10 h) or by cell viability detection at different time intervals.

Further experiments, in which *E. coli* strains, transformed with either pBAD42 cloned with *cptBA* cassette (in the same syntenic order as its order on *A. baumannii* chromosome) or with the corresponding empty plasmids, were carried out as follows. Cells were cultured overnight in LB broth, which had been supplemented with 50 μg/ml streptomycin and diluted 1:100 in fresh medium. Afterward, culture growth under 0.2% L-arabinose induction was monitored by OD_{600nm} measurement and viable count by the plate dilution method.

Microscopic examination

To prepare samples for microscopy, we diluted overnight cultures to reach an OD600nm ~0.04 in fresh LB broth, supplemented with the appropriate antibiotic (apramycin or streptomycin). Induced cells were incubated at 37 °C with shaking at 180 rpm, heat fixed, simple-stained by crystal violet, and examined under an Olympus CH20BIMF200 microscope (Olympus optical co., Japan) at different time points.

In addition, samples in which the toxin gene was induced (with 0.2% arabinose) were analyzed under a JEOL-JEM 1010 transmission electron microscope (The Regional Center for Mycology and Biotechnology, Al-Azhar University).

Determination of the optimal level of IPTG required to induce CptB expression

Overnight cultures of *E. coli* BL21(DE3) strains, whether harboring the dual promoter pBAD18-*cptA-cptB-*P_{T7} vector or the empty pBAD18 ori, were diluted by fresh LB broth, supplemented with 50 μg/ml apramycin, to OD_{600nm} ~0.04. In case of BL21(DE3) cells harboring the dual promoter pBAD18-*cptA-cptB-*P_{T7} vector, the culture was divided into eight equal parts (4 ml each), of which five were supplemented with different concentrations of IPTG (0.01, 0.1, 1, 5 and 10 mM); the sixth part was supplied with 0.2% L-arabinose; while the last two parts were used as controls—with no inducer added. After two hours of incubation at 37 °C with shaking at 180 rpm, 0.2% L-arabinose was added to the previously induced IPTG tubes as well as to one of the uninduced control tubes, and then re-incubated under the same conditions. Culture growth was assessed by measuring OD_{600nm} for up to 8 h.

Testing for CptB antagonism of CptA

Overnight cultures of BL21(DE3) cells, whether harboring the dual promoter pBAD18-*cptA-cptB-*P_{T7} vector or the empty pBAD18 plasmid, were diluted by fresh LB broth, supplemented with 50 μg/ml apramycin to OD_{600nm} ~0.04. The BL21(DE3) culture harboring the dual promoter pBAD18-*cptA-cptB-*P_{T7} vector was divided into five equal parts, of which one was left as a control, then each other two parts were supplemented with either 5 mM IPTG or 0.2% L- arabinose and left to grow for three hours; then the reverse inducer was added. The cultures were allowed to grow at 37 °C, with shaking at 180 rpm, for 8 h, and samples were collected every hour from each culture for OD_{600nm} measurement, and every 2 h for viable count determination by the serial dilution method.

Statistical analysis

All statistical analyses were performed with GraphPad Prism 5 (GraphPad Software, San Diego, USA). For experiments involving multiple variables, we used Analysis of Variance (ANOVA), followed by *post hoc* multiple *t*-tests, with Holm-Sidak correction. For two variable comparisons, Student's *t*-test was used to determine the significance of the differences between means. In all tests, a *p*-value of < 0.05 was considered a statistically significant difference between the compared means or variables.

Results

The goal of this study was to explore novel TA systems in the multiresistant *A. baumannii* bacteria to exploit them, on the long term, as potential alternative antimicrobial targets.

The A. baumannii ATCC 17978 genome contains potential TA systems

When the *A. baumannii* ATCC 17978 genome was computationally screened against the TADB online resource, only five type II TA systems were pre-identified, but no type IV system was found in this organism. Overall, TADB only lists four type IV TA systems: the *cptA*/*cptB* and *yeeV*/*yeeU* systems in *E. coli* str. K-12 substr. MG1655 (chromosome), the *abiGI*/*abiGII* system in *Streptococcus agalactiae* 2603 V/R (chromosome), and the *abiEI*/*abiEII* system in *Lactococcus lactis* (plasmid pNP40). Thus, we manually screened the genome of *A. baumannii* standard strain ATCC 17978 against each of these four systems, and the only significant match was to the CptA/CptB system in *E. coli*, which was subsequently found to be conserved in *A. baumannii*, as detailed below.

The two matched proteins had relatively small sizes of 129 and 85 amino acids. Their homology to the *E. coli* system was confirmed by BLASTP, based on 22.94% sequence identity to CptA (129 amino acids, with 79% coverage and E-value = 0.018) and 33.87% identity to CptB (85 amino acids, with 72% coverage and E-value = 10^{-14}). Additionally, maximum likelihood phylogenetic analysis for both CptA and CptB delineated two major groups, in each of which *Acinetobacter* spp. clustered together (Fig. 1). Moreover, multiple sequence analysis revealed the conservation of *cptBA* in 195 representative strains of *A. baumannii* (in the SEED database [25]) in the same syntenic order, where the antitoxin genes preceded those of the toxin (see representative contextual alignments Fig. S1). For updates, *A. baumannii* genomes in NCBI RefSeq database were frequently screened by tBLASTN, lastly on November 15, 2020, and 4732 out of all 4759 *A. baumannii* genomes in RefSeq (99.4%) were found to have the intact system in a syntenic order as well.

Since the *E. coli* toxin, CptA, is a transmembrane protein, the subcellular localization and topology of the *A. baumannii* homolog was investigated by the TMHMM tool of the CCTOP server. The protein was indeed predicted to be a transmembrane protein and had similar orientation through the inner membrane to that of the *E. coli* toxin (Fig. S2**)**. Hereafter we will refer to this locus as *cptBA* and to its encoded proteins as CptB and CptA. The *cptBA* genetic locus in *A. baumannii* is surrounded by unannotated regions of 187 bp and 769 bp upstream *cptB* and downstream *cptA*, respectively (Fig. S3A).

A. baumannii cptBA-like TA genes are co-transcribed

Since the in silico analysis of the *cptBA* locus in *A. baumannii* ATCC 17978 strain indicated that both genes are oriented on the same strand, and that the antitoxin is directly upstream to the toxin, we investigated their transcriptional orientation. Reverse transcription-PCR (RT-PCR) of each of the two genes individually indicated their transcription, while RT-PCR amplification spanning their junction indicated that they are transcribed as one polycistronic message (Fig. S3B).

Construction of a set of dual-promoter vectors allows studying the TA encoding genes under the control of different inducers

To better understand the function of *cptBA* and its gene products, we set out to clone and express the gene pair in a heterologous host, *E. coli*, and conduct gain of function studies to analyze the effect of the expressed genes, as well as the time and order of their expression, on the growth of the bacterial host.

To this end, we constructed a dual-promoter vector, pBAD18-*cptA-cptB-*P_{T7}, so that the *cptA* gene (toxin) would be under the control of the arabinose-inducible promoter *pBAD* while the *cptB* gene (antitoxin) under the IPTG-inducible promoter $P_{T7,}$ as illustrated in Fig. S4. In addition, the TA system was cloned, with in the same syntenic order, in pBAD42 vector resembling their orientation in the *A. baumannii* chromosome, where the antitoxin precedes the toxin. (All maps and PCR results that confirm the correct orientations are shown in supplementary Figs. S5 to S11).

Toxin induction in a heterologous host leads to drastic decrease in growth

When BL21(DE3) *E. coli* cells harboring pBAD18-*cptA-cptB-*P_{T7} were treated by 0.2% L- arabinose to induce the *cptA* toxin gene, a significant and drastic decrease of their growth rate was observed. This decrease was statistically significant ($p < 0.05$, ANOVA followed by *post hoc t*-test) at time points ranging from 4 to 10 h relative to the wild type, the different controls, and even to the IPTG-induced cells for antitoxin gene (*cptB*) expression

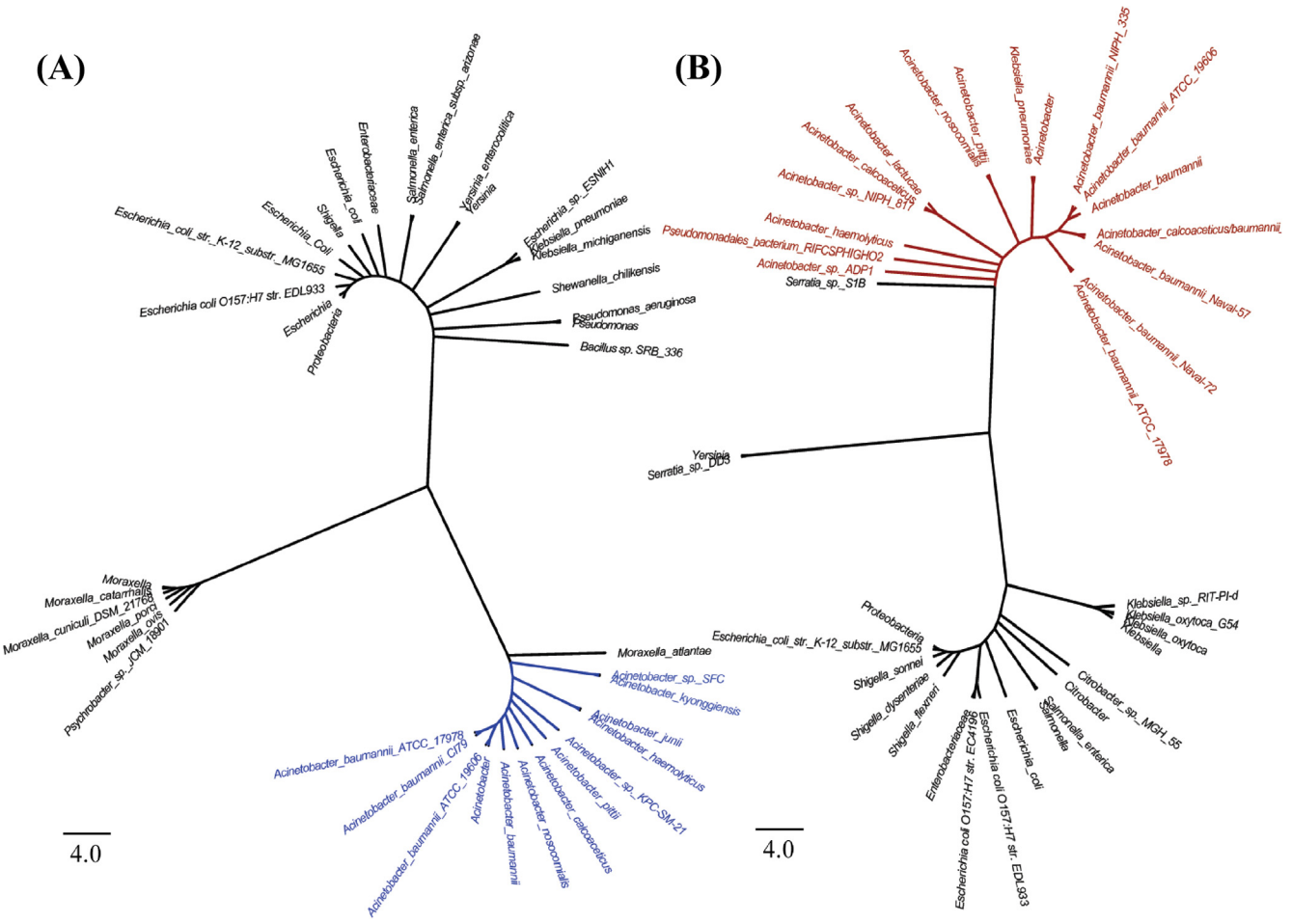

Fig. 1. Maximum likelihood phylogenetic analysis of CptA and CptB. Maximum likelihood phylogenetic trees of 39 and 37 protein sequences of the candidate antitoxin (A) and toxin (B), respectively. Candidate *Acinetobacte*r spp. antitoxins are highlighted in blue, while candidate toxins are highlighted in red. Their homologs in other species are represented in black. The analyses were conducted by the MEGA X software, where all positions with less than 95% site coverage were eliminated (i.e., fewer than 5% alignment gaps).

(Fig. 2A). In addition, we also confirmed the association of growth reduction with a decrease in viable cells by comparative viable count experiments, in which the cell counts followed the same pattern as with growth experiments (Fig. 2B).

On the other hand, when *cptB* expression was induced by 1 mM IPTG, no significant effect on the growth rates, nor the viable counts, was observed at any time point (Fig. 2). These findings highlighted that *A. baumannii cptA* expression is toxic to *E. coli* cells, suggesting it might indeed be a toxin, similar to its *E. coli* homolog.

Toxin production in E. coli is accompanied by morphological change

Next, we questioned whether *A. baumannii cptA* expression would induce morphological aberrations in *E. coli* especially it is known that *E. coli* CptA toxins usually induce drastic morphological changes to bacterial cells. Microscopic examination of BL21(DE3) cells, harboring pBAD18-*cptA*-*cptB*-P_{T7}, after 10 h of induction by IPTG or L-arabinose revealed that cells with overproduced CptA (arabinose-induced) tend to filament (Fig. 3C). Some of the arabinose-induced cells changed even more, after 10 and 24 h of induction, to become lemon shaped (Fig. 3D). By contrast, uninduced (Fig. 3A) and IPTG-induced (Fig. 3B) cells kept their usual rod shape. Further investigation using transmission electron microscopy showed elongated filament-shaped cells with no signs of division or DNA replication in arabinose-induced cells (Fig. 3F), in contrary to uninduced cells, which showed two copies of DNA in their way to divide, like any normal-growing cells (Fig. 3E).

Toxin effect predominates over that of antitoxin at lower levels of induction

To investigate the antitoxin-antagonizing activity against the toxin, we induced *cptB* expression using 1 mM IPTG. We did not observe any effect on the growth of the cells induced by 0.2% L-arabinose for *cptA* expression, regardless of the time of antitoxin induction (Fig. S12). This experiment suggested that 1 mM induction of *cptB* was not sufficient to counteract the effect of CptA, and that time of induction may not be the only factor, but perhaps the concentration as well.

Antitoxin protection effect is concentration and time dependent

To further investigate *A. baumannii* CptB antitoxin's effect against its cognate toxin CtpA, we induced *cptB* at different times and with higher concentrations of IPTG. *E. coli* BL21(DE3) cells, transformed with pBAD18-*cptA*-*cptB*-P_{T7}, were subjected to different levels of antitoxin induction (IPTG 0.01, 0.1, 1, 5 and 10 mM) followed by a constant level of 0.2% L-arabinose for toxin induction. At low concentration of IPTG (0.01–1 mM), the antitoxin failed to protect the cells against the toxin (Fig. 4A).

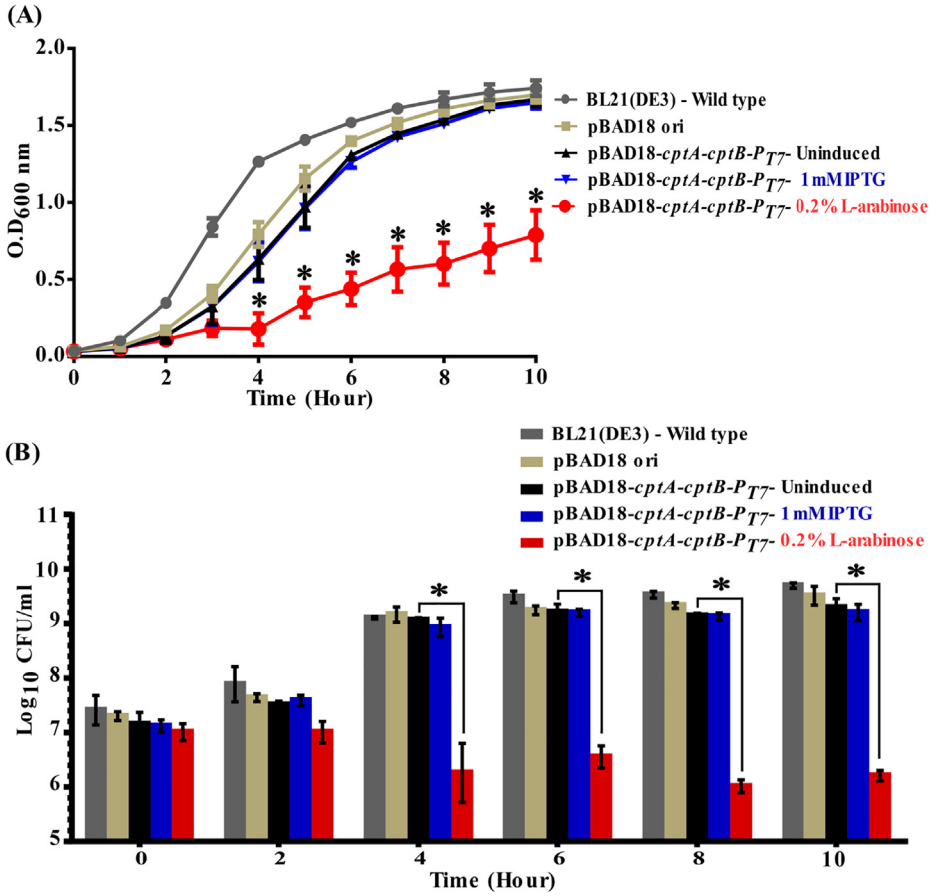

Fig. 2. Effect of inducing *A. baumannii* CptA and CptB on the growth of *E. coli*. (A) Growth curves of *E. coli* Bl21(DE3) cells harboring the dual promoter plasmid pBAD18-*cptA-cptB*-P_{T7}, induced by either 0.2% L-arabinose (CptA inducer) or IPTG 1 mM (CptB inducer) *vs.* uninduced cells, those carrying pBAD18 ori (control vector), and the untransformed wild-type bacterial cells. Samples were drawn every hour for 10 h. (B) Bar chart representing the viable counts of *E. coli* Bl21(DE3) cells carrying pBAD18-*cptA-cptB*-P_{T7} upon induction with 0.2% L-arabinose or IPTG 1 mM, compared to uninduced cells, those with vector alone (pBAD18 ori), and untransformed wild-type cells. Viable counts samples were collected at different time points, serially diluted and plated on either LBA or LBA with apramycin. The viable counts were calculated as CFU/ml and Log_{10} data plotted against time. The data represent the means of three independent experiments. The error bars represent the standard error of the means. Asterisks (*) indicate statistically significant differences (at $p < 0.05$), in comparison to uninduced cells as determined by ANOVA followed by *post hoc t*-test.

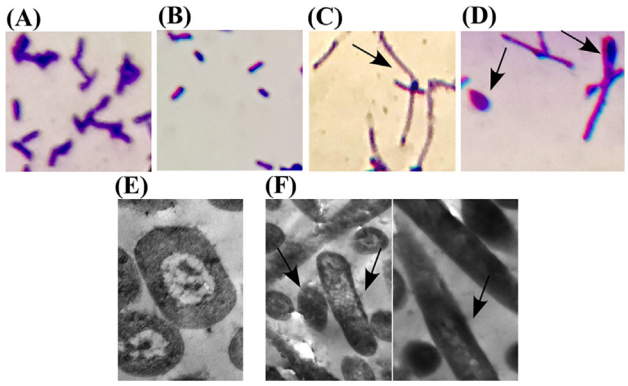

Fig. 3. Microscopic examination of morphological changes upon toxin induction in *E. coli*. (A-D) Light micrographs representing crystal violet-stained *E. coli* Bl21(DE3) cells with the dual promoter plasmid pBAD18-*cptA-cptB*-P_{T7}. (A) Uninduced cells serve as control; (B) cells induced with 1 mM IPTG; (C) cells induced with 0.2% L-arabinose after ten hours of induction; and (D) same cells as in (C) after 24 h of 0.2% L-arabinose induction. L-arabinose-induced cells, expressing toxin but no antitoxin, appear (C) filamented and (D) lemon-shaped. Both control (A) and antitoxin-expressing cells (B) kept the typical rod-shaped form of *E. coli*. (E-F) Electron micrographs of uninduced and L-arabinose induced cells. (E) Uninduced cells serve as control with rod-shaped cells showing two copies of DNA as a step towards binary fission; (F, both panels) 0.2% L-arabinose induced cells in which cells tend to filament under the effect of toxin induction with no signs of cell division, but with (F, right panel) some lemon-shaped cells instead of dividing rods.

On the contrary, higher levels of antitoxin, induced by 5 and 10 mM IPTG showed a considerable protection effect against toxin (Fig. 4A). Induction of higher levels of antitoxin provided the same growth rate as uninduced cells, but had significantly higher growth rates when compared to cells induced by L-arabinose only (i.e., only producing toxin). Such a pattern suggests that prior induction of antitoxin with higher concentration of IPTG (5–10 mM *vs.* 0.01–1 mM) protected the cells from the CptA-driven growth reduction.

Beside the ability of the antitoxin to protect the cells prior to toxin expression, we reasoned that the antitoxin effect on the toxin can be exerted in two other ways (that are not necessarily mutually exclusive with its protection ability): (i) competition on the same molecular target or (ii) reversal or neutralization of the toxin- induced lethality. Accordingly, we tested these two possibilities by either the simultaneous co-induction of the *cptA* and *cptB*, or the induction of *cptA* before *cptB*, respectively.

Simultaneous induction of both antitoxin and toxin with 5 mM IPTG and 0.2% L-arabinose, respectively, showed significant but moderate increase in growth rate relative to the toxin induced cells only (Fig. 4B), suggesting that CptA and CptB might compete for the same molecular target. This result also suggests that the antitoxin growth rescue is concentration dependent since it was not observed upon co-induction with 0.2% L-arabinose and 1 mM IPTG (Fig. S12A). This observation was confirmed by: i) a significant increase in the percent survival of cells induced by 5 mM IPTG

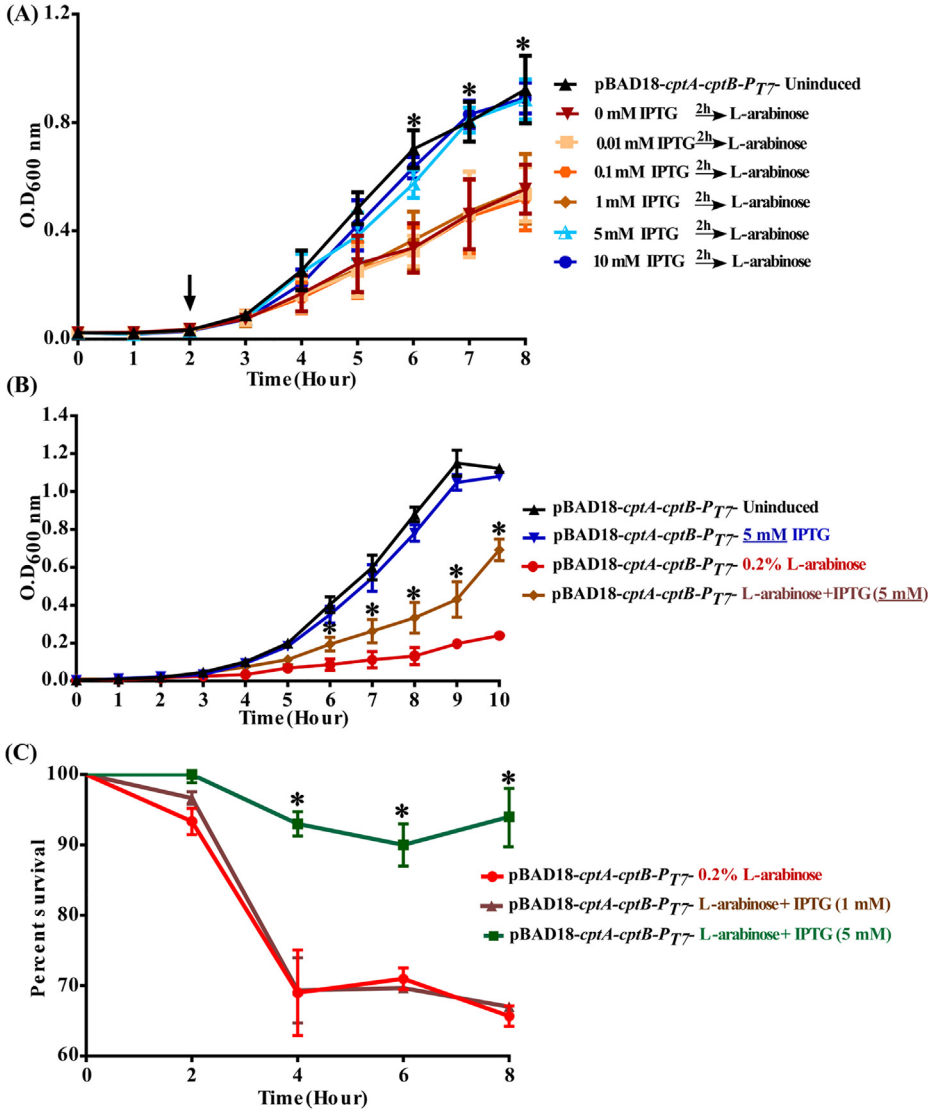

Fig. 4. Different levels of the CptB antitoxin showed diversity in its protection effect against the CptA toxin. Growth curves and percentage of surviving viable cells of *E. coli* Bl21(DE3) harboring the dual promoter plasmid pBAD18-*cptA-cptB-*P_{T7} *vs.* uninduced cells (control) at the following conditions. (A) antitoxin induction using different concentrations of IPTG (0.01, 0.1, 1, 5 and 10 mM), followed by toxin induction (0.2% L-arabinose) *vs* cells with L-arabinose induction only, (B) induction by either 0.2% L-arabinose (CptA inducer), 5 mM IPTG (CptB inducer), or both. OD_{600nm} was measured every hour for 10 h. (C) Percentage of surviving viable cells upon simultaneous induction of both toxin (with 0.2% L-arabinose) and antitoxin (with either 1 or 5 mM IPTG). Percent survival was calculated using viable count assays, and plotted against time. The data represent the means of three independent experiments. Error bars represent the standard error of the means. Asterisks (*) indicate statistically significant differences (at $p < 0.05$), as determined by ANOVA followed by *post hoc t*-test.

vs. those induced by 1 mM IPTG (20–27%, $p < 0.05$, Fig. 4C); ii) a significant increase in *cptB* mRNA levels in cells induced by 5 mM IPTG *vs.* those induced by 1 mM IPTG (13.89 fold increase, $p = 0.0285$) (data not shown).

On another front, pre-induction of the antitoxin by 5 mM IPTG successfully blocked the toxicity of the toxin, induced two hours later (by 0.2% L-arabinose). This blocking effect was demonstrated by the restoration of *E. coli* growth rate (Fig. 5A), as well as the increase of their survival, in comparison to cells in which only the toxin was induced (Fig. 5B). However, induction of the antitoxin three hours after the toxin induction did not reverse the growth reduction (Fig. 5C) or the survival (Fig. 5D) of the toxin-induced cells, even with 5 mM IPTG.

Taken together, these results suggest that CptB can either protect *E. coli* cells from CptA (in case of *cptB* induction before *cptA*) or can partially prevent its effect (upon co-induction). However, CptB could not rescue the lethal effect of CptA.

We further cloned the *cptBA* cassette, in which the antitoxin (*cptB*) was located upstream the toxin gene (*cptA*), into pBAD42 and then transformed it in BL21(DE3), forcing the two genes to be transcribed by the same promoter. In this case, the co-production of TA together showed only slightly significant decrease in the growth rate after 6 h of L-arabinose induction (Fig. S13). This observation may emphasize the higher stability of the toxin protein even when both genes are simultaneously transcribed and could possibly be overcome by higher transcription of the antitoxin gene.

cptBA transcription in its native bacterial host (A. baumannii) varies under selected stress factors

Given the reported role of CptBA and its homologs in stress response in *E. coli* and other bacteria, we investigated the tran-

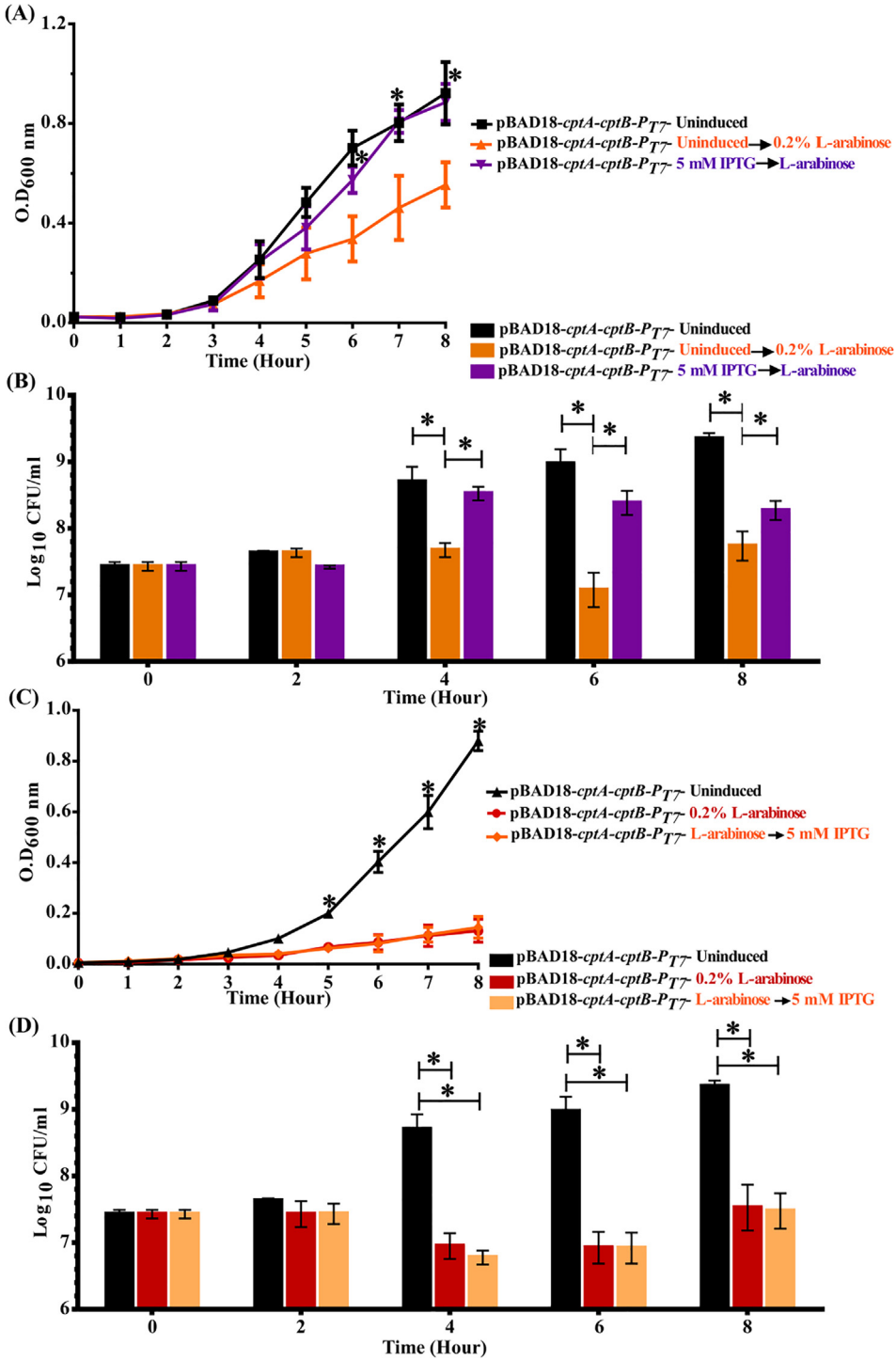

Fig. 5. Effect of pre- and post-induction of *A. baumannii cptB* antitoxin to the *A. baumannii* CptA toxin expression on the growth of *E. coli.* (A) Growth curves and (B) viable count bar charts of *E. coli* Bl21(DE3) harboring the dual promoter plasmid pBAD18-*cptA-cptB-*P_{T7} *vs.* uninduced cells (control) upon induction of antitoxin expression (5 mM IPTG) prior to toxin expression; whereas (C) growth curves and (D) viable count bar charts represent the induction of toxin expression (0.2% L-arabinose) prior to that of the antitoxin. OD_{600nm} was measured every hour for 8 h, and plotted against time. Viable counts were sampled at different time points, serially diluted and plated on LB agar with apramycin. The viable counts were calculated as CFU/ml and Log_{10} data plotted against time. The data represent the means of three independent experiments. Error bars represent the standard error of the means. Asterisks (*) indicate statistically significant differences (at $p < 0.05$) between induced and uninduced cells, as determined by ANOVA followed by *post hoc t*-test.

scription of *cptBA* under different stresses, including antibiotic exposure.

Testing different classes of antibiotics had different effects on *cptBA*: ciprofloxacin led to a significant downregulation of both *cptA* and *cptB* by 5.26 and 4.48 folds, respectively, compared to the non-antibiotic-treated cells (Fig. 6A). Nevertheless, other antibiotics, including meropenem, significantly reduced *cptA* and *cptB* levels by 3.2 and 2.23 folds, respectively (Fig. 6A),

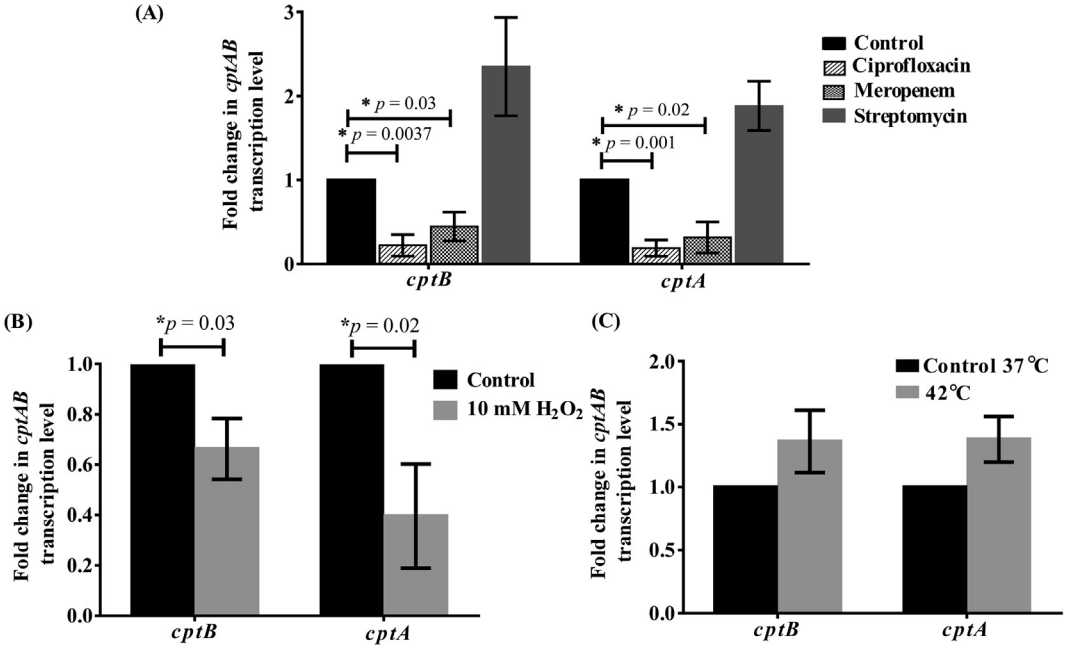

Fig. 6. Expression of CptBA system varies under different stressful conditions in *A. baumannii* ATCC 17978. Fold change in the transcription levels of *cptA* and *cptB* genes upon exposure to (A) different antibiotics, (B) oxidative stress and (C) high temperature (42 °C *vs* 37 °C). Significant downregulation was observed in *cptBA* under the effect of 10 mM H_2O_2, and in the presence of ciprofloxacin (32 μg/ml) and meropenem (32 μg/ml). Fold change was calculated using the ΔΔCt method. The data represent the means of three independent experiments. The error bars represent the standard error of the means. Asterisks (*) indicate statistically significant differences (at $p < 0.05$), as determined by the unpaired Student's *t*-test.

while the protein synthesis-inhibiting antibiotic, streptomycin, had no statistically significant effect (Fig. 6A). Moreover, upon exposure to oxidative stress, both genes were significantly ($p < 0.05$) downregulated (*cptA* by 2.5 folds and *cptB* by 1.5 folds) relative to their expression levels in unexposed bacteria (Fig. 6B); however, no significant effect on both on *cptA* and *cptB* was observed upon *A. baumannii*'s exposure to 42 °C (Fig. 6C). The downregulation of *cptBA* transcription was accompanied by an expected growth reduction upon exposure to different antibiotics and oxidative stresses, but not 42 °C temperature (Fig. S14).

To validate these findings on clinical isolates, we conducted similar transcriptional studies, with the stress factors that significantly affected the standard strain, on three clinical *A. baumannii* isolates, AB01, AB02, and AB03. Like with *A. baumannii* ATCC 17978 standard strain, the *cptBA* transcription of the three clinical isolates was significantly downregulated upon exposure to oxidative stress.

When treated with 10 mM H_2O_2., AB01 had significant reduction in the transcriptional level of *cptA* by 12.5 folds and *cptB* by 2.1 folds (Fig. S15A). Likewise, a significant decrease was observed in the transcript levels of *cptA* (by 5.6 folds) and *cptB* (by 2.8 folds) in AB02 (Fig. S15B). Similarly, AB03 *cptA* transcription was significantly reduced by 5.3 folds together with a significant decrease of *cptB* transcription by 1.4 folds (Fig. S15C).

For antibiotic stress, AB01 and AB02 were sensitive to ciprofloxacin and meropenem, whereas AB03 was resistant to both antibiotics, so the effect of these two antibiotics was only tested on AB01 and AB02. In AB01, ciprofloxacin led to a significant decrease in *cptA* and *cptB* transcription by 37 and 11 folds, respectively (Fig. S15D). Similarly, in AB02, ciprofloxacin decreased *cptA* and *cptB* transcription by 5.55 and 18.8 folds, respectively (Fig. S15E). For meropenem, *cptA* and *cptB* transcript levels were reduced by 2.8 and 5 folds in AB01, and by 2.5 and 3.1 folds in AB02, respectively (Fig. S15D and E).

Discussion

The rise and expansion of microbial genomics provided unprecedented wealth of information on microbial genes and their functions; yet the accumulation of genome sequences surprisingly unveiled how much information remains unknown. Indeed, at least 40% of bacterial genes remain with no assigned functions [25] and are sometimes collectively known as the 'biological dark matter' [28]. Many of these unknown genes are often those that differentiate strains within same species, and endow bacteria with fitness advantages through phenotypes like virulence, biodegradation, antimicrobial resistance, or immune evasion. Comparative genomics and genome-scale models, combined with genetic screens and molecular experiments, allow better phenotype-genotype correlations through assignment of functions to those genes—aided by computational predictions, constituting a rapidly growing field of research known as 'gap filling' [29].

Among the genes that are harder to decipher in bacterial genomes are genes encoding surface proteins that are under positive selection pressure, genes from mobile elements, such as prophage and transposase genes [30], and other specific genetic elements such as CRISPRs and toxin-antitoxin (TA) systems.

TA systems are widely spread among bacteria and archaea, and have been well-studied in model pathogens, such as *E. coli* and *M. tuberculosis*. The highest number of TA loci (>60) are defined in *M. tuberculosis*, where they are thought to be correlated with its pathogenic nature (*vs.* other mycobacteria) by maintaining the bacteria inside macrophages while being in a dormant state [31]. *E. coli* K-12 MG1655, the model organism for Gram-negative bacteria, is known to encode 35 putative TA system, including 19 type I, 13 type II and three type IV systems [32].

Despite the distribution of this large family of TA systems among microorganisms, they remain poorly characterized in many bacteria with public health implications, such as *A. baumannii*, which is the focus of this study. Missing information about TA sys-

tems in *A. baumannii* include whether they are chromosomal or on plasmids, and whether they lead to antibiotic treatment failure by contributing to antibiotic-tolerance in persister cells, which may eventually cause infection relapse [18].

Most of the TA systems that had been identified in *A. baumannii* belong to type II, but no type IV TA systems have been defined, to the best of our knowledge. Using a combination of in silico and *in vitro* strategies, this work identified a type IV CptBA-like TA system in *A. baumannii*. This specific system is well characterized in non-pathogenic *E. coli*; yet little is known about its distribution among other organisms, especially pathogens. Using different bioinformatic tools, we demonstrated a wide distribution of CptBA-like systems among Gram-negative bacteria. This distribution and conservation among different organisms make CptB and CptA suitable drug target candidates with a relatively broad spectrum. Alternatives for conventional antibiotics are continually sought, especially that *A. baumannii* is among the major multidrug-resistant organism [33].

Although the *E. coli* CptA protein is only moderately similar at the sequence level (22.8%) to its corresponding toxin in *A. baumannii*, they both share similar topology as transmembrane proteins, which is one of the characteristics of this family's toxins, indicating similar function [5]. Additionally, the conserved synteny of the genes encoding both proteins supports their functional dependence, as toxin genes alone would be lethal to the cells carrying them. This lethality exerts selective pressure on both genes to remain contiguous and to be co-transcribed, which we demonstrated experimentally (Fig. S3), or else cells with toxin alone will eventually perish. Further evidence is provided by the small size of the encoded proteins (129 and 85 amino acids), which is typical of many protein TA systems [1,34]. Of note, the syntenic conservation of both CptA and CptB in 4,732 (99.4%) *A. baumannii* genomes also reflects that the presence of the toxin gene is advantageous to the bacteria, since it was not lost in spite of the lethality of its product. It is not clear whether the few genomes (27 out of 4759), in which the two genes were not detected in syntenic order, truly lack the genes or were related to sequencing or assembly issues (multiple contigs of small size, repeated contigs, or low coverage).

Bioinformatics analysis greatly helps formulating reasonable hypotheses and cuts short the time of trial and error while screening for gene functions; however, experimental substantiation remains imperative. Effectively, subsequent experimental findings of this study bolstered the hypothesis that the chromosomally encoded *cptBA* locus of *A. baumannii* is an active TA system, with *cptA* encoding the toxin and *cptB* encoding its cognate antitoxin. Overproducing the *cptA* gene product in *E. coli* BL21(DE3) cells resulted in severe inhibition of bacterial growth, accompanied by morphological changes from rod-shaped to elongated filament-shaped cells, which changed by time to a lemon-shaped morphology. This morphological change is congruent with earlier reports that initially identified CptA in *E. coli* as a cytoskeleton polymerization-inhibiting toxin A, that inhibits FtsZ and MreB polymerization, thus inhibiting cell division and producing a distinct morphological change to elongated-shaped and lemon-shaped cells [5].

The toxic effect of CptA was demonstrated, not only by its severe inhibition of bacterial growth, but also by its ability to reduce cell viability by about 1000 folds. The toxic effect of CptA could be neutralized by its cognate antitoxin only when the latter was induced by higher levels of IPTG (5–10 mM *vs.* $\leq$1 mM). This finding highlights the importance of having sufficient levels of pre-made antitoxin proteins to overcome the toxicity of CptA. We mainly attribute this to the unstable nature of the antitoxin relative to that of the toxin, which justifies the inability of low levels of the easily degradable antitoxin to overcome the toxin activity upon co- or pre-induction with usual level of IPTG (1 mM). We therefore reasoned that the antitoxin activity is concentration and time dependent, and such assumption was experimentally confirmed (Figs. 4 and 5). Even with simultaneous induction of the toxin and antitoxin, only cells with highly induced antitoxin (CptB) were protected from the growth-reducing effect of the toxin (CptA).

Both the concentration and timing of antitoxin induction (pre- or with the toxin induction) could be considered vital for its function. However, post CptB induction, even with higher IPTG levels, could not reverse the preceded toxic effect of CptA. This result agrees with what is known about the nature type IV TA systems, whose mechanism relies on the toxin-antitoxin competition for the same target, though they never interact. As a consequence, once the toxin is produced, it binds to and inhibits the polymerization of the bacterial cytoskeletal proteins, MreB and FtsZ, thereby blocking cell division and, hence, preventing multiplication. At that point, the antitoxin cannot antagonize the toxin activity; instead, it can promote and stabilize MreB and FtsZ cytoskeletal filament bundling if produced at earlier stage before the toxin production [4,35].

When both CptB and CptA were simultaneously induced under the control of a single promoter (arabinose), an unexpected slight decrease in the growth rate of the transformed bacteria was observed, but this decrease appeared late, after 6 h of induction, without any change in cellular morphology or cell viability. We related that late slowdown in growth to the remaining effect of the more stable toxin *vs.* the labile antitoxin after the system's induction was stopped. However, such decrease was not accompanied by morphological changes, as cells had already bypassed the exponential phase (Fig. S13). Thus, we concluded that two factors would determine which of the two proteins will reach and saturate its target: (i) stability, (ii) target accessibility as determined by speed and amount of production. In other terms, the first produced protein (either toxin or antitoxin) that will reach its target in high amounts will temporarily predominate; yet the more stable protein will be the one to prevail in the end. In this case, large amounts of antitoxin proteins may saturate their target for a while, but as they degrade faster than toxin proteins, the latter will gradually replace them and lead to growth reduction, unless more antitoxin is produced.

In summary, gain-of-function studies on the *A. baumannii cptBA*-like genetic locus, by inserting that locus in *E. coli* and inducing it simultaneously (under control of arabinose promoter) then differentially under two different promoters, demonstrated that *cptB* expression was able to reverse *cptA* growth inhibition. Thus, we propose this system as a new type IV TA system in *A. baumannii*.

It remained important to study the transcription of that system in *A. baumannii* under different stress conditions, like antibiotic stress, oxidative stress (10 mM H_2O_2), and high temperature (42 °C). Because of the pronounced role of TA systems in persister cell formation, and because some antibiotics were reported to trigger cell death indirectly through mediating TA systems, we studied the effect of different classes of antibiotics on *cptBA* expression in *A. baumannii* [19,36]. Ciprofloxacin, a DNA gyrase inhibitor, significantly reduced *cptBA* transcription level, accompanied by a significant decrease in growth rate of *A. baumannii* (Fig. S14A). One possible mechanism that remains to be further explored is that the reduction of CptA and CptB levels affects the homeostasis of the TA system, thereby permitting the lethal action of the toxic protein in the absence of a considerable level of the labile antitoxin. Such mechanism has been reported for MazEF TA system and is consistent with the results of our gain-of-function studies in BL21(DE3) cells.

Meropenem, a beta lactam, was selected for its cell wall inhibition mechanism that requires a growing cell, resembling the confirmed CptA toxin function affecting the polymerization of FstZ

and MreB, and thus affecting cell division. Meropenem significantly downregulated *cptBA* transcription, in parallel to a significant decrease in growth rate of *A. baumannii* cells (Fig. S14A). However, not all antibiotics had a similar effect. For example, with the protein synthesis inhibitor, streptomycin, *cptBA* transcription was not significantly affected.

Like ciprofloxacin and meropenem, oxidative stress, reported by Juttukonda and coworkers [37] to decrease *A. baumannii* viability, led to transcriptional downregulation of *cptBA* (Fig. 6A-B). We speculated that such decrease in *A. baumannii* growth upon exposure to ciprofloxacin, meropenem, as well as hydrogen peroxide (Fig. S14A-B) could be attributed to the disruption in the homeostatic level of CptBA level, similar to what was reported by Narisima and coworkers [38] about the downregulation of different TA systems in *Klebsiella pneumonia* under oxidative and antibiotic stresses. In that study, Narimisa and coworkers [38] correlated the downregulation of type II TA systems under different stresses with the rapid degradation of the labile antitoxins, which caused a sudden relative increase in the free stable toxins, eventually leading to cell death. Hence, the stable nature of the toxin protein predominated over the labile antitoxin, in agreement with cases of post-segregation killing, in which cells losing the TA-encoded plasmids die by toxin effect in the absence of continuous production of its antidote [39,40]. Based on the above, we suggest that the chromosomal *A. baumannii* CptBA-encoding genes could have an inherent role in inducing programmed cell death upon exposure to different unfavorable conditions.

The above stresses were first investigated in the standard *A. baumannii* ATCC 17978 strain, because its full genome sequence is available, which allowed the design of unambiguous primers and the confirmation that no other paralogs of these genes could confound the results. However, it is quite common that clinical isolates behave differently from those strain that were deemed 'standard' because they were being studied in the laboratory for years. Consequently, we investigated the effect of those stressors that significantly affected ATCC 17978 in three clinical isolates. All three isolates responded similarly to oxidative stress, and the two of them that were sensitive to ciprofloxacin and meropenem responded similarly to suprainhibitory concentrations of these two antibiotics (Fig. S15). Obviously, studying the effect of these two antibiotics in a resistant isolate is unrelated to the hypothesis that they may be exerting their function, at least partially, through CptBA.

Conclusion and outlook

We provide computational and experimental evidence that *A. baumannii* CptBA is a TA system, most likely acting with type IV mechanism. The transcription of this system was downregulated by oxidative stress and some antibiotics, and its role in bacterial virulence should be investigated in future studies.

This novel TA system in *A. baumannii* could be considered among potential drug targets for this resistant pathogen that causes serious nosocomial infections. This could be done either by targeting the labile antitoxin or targeting the toxin itself to promote intracellular cell suicide. Moreover, targeting of TA promoter could lead to disruption in toxin-antitoxin balance, and therefore give the opportunity for the stable released toxin to undergo cell death.

Understanding the spread and distribution of different TA systems among bacteria opens the gate for using them as new non-antibiotic therapeutic targets. Thus, future studies concerning the investigation and the characterization of new TA systems are necessary.

Compliance with Ethics Requirements

This article does not contain any studies with human or animal subjects.

Declaration of Competing Interest

The authors declare that they have no known competing financial interests or personal relationships that could have appeared to influence the work reported in this paper.

Acknowledgments

We thank the following individuals for sharing cells or reagents: Dr. Ahmed S. Attia (*A. baumannii* standard strain); Dr. Nahla Hussein (*E. coli* XL-1 Blue cells and pBAD42 plasmid); Dr. Noha M. Elhosseiny (*E. coli* Bl21(DE3) cells and pBAD18 ori). The graphical abstract was created with BioRender.com and SnapGene® viewer software.

Appendix A. Supplementary material

Supplementary data to this article can be found online at https://doi.org/10.1016/j.jare.2020.11.007.

References

[1] Unterholzner SJ, Poppenberger B, Rozhon W. Toxin-antitoxin systems: Biology, identification, and application. Mob Genet Elements 2013;3(5):. doi: https://doi.org/10.4161/mge.26219e26219.
[2] Hazan R, Sat B, Engelberg-Kulka H. *Escherichia coli mazEF*-mediated cell death is triggered by various stressful conditions. J Bacteriol 2004;186(11):3663–9. doi: https://doi.org/10.1128/JB.186.11.3663-3669.2004.
[3] Wen Y, Behiels E, Devreese B. Toxin-antitoxin systems: Their role in persistence, biofilm formation, and pathogenicity. Pathog Dis 2014;70(3):240–9. doi: https://doi.org/10.1111/2049-632X.12145.
[4] Masuda H, Tan Q, Awano N, Wu KP, Inouye M. YeeU enhances the bundling of cytoskeletal polymers of MreB and FtsZ, antagonizing the CbtA (YeeV) toxicity in *Escherichia coli*. Mol Microbiol 2012;84(5):979–89. doi: https://doi.org/10.1111/j.1365-2958.2012.08068.x.
[5] Masuda H, Tan Q, Awano N, Yamaguchi Y, Inouye M. A novel membrane-bound toxin for cell division, CptA (YgfX), inhibits polymerization of cytoskeleton proteins, FtsZ and MreB, in *Escherichia coli*. FEMS Microbiol Lett 2012;328(2):174–81. doi: https://doi.org/10.1111/j.1574-6968.2012.02496.x.
[6] Lobato-Marquez D, Diaz-Orejas R, Garcia-Del Portillo F. Toxin-antitoxins and bacterial virulence. FEMS Microbiol Rev 2016;40(5):592–609. doi: https://doi.org/10.1093/femsre/fuw022.
[7] Rowe-Magnus DA, Guerout AM, Biskri L, Bouige P, Mazel D. Comparative analysis of superintegrons: Engineering extensive genetic diversity in the Vibrionaceae. Genome Res 2003;13(3):428–42. doi: https://doi.org/10.1101/gr.617103.
[8] Hazan R, Engelberg-Kulka H. *Escherichia coli mazEF*-mediated cell death as a defense mechanism that inhibits the spread of phage P1. Mol Genet Genomics 2004;272(2):227–34. doi: https://doi.org/10.1007/s00438-004-1048-y.
[9] Yamaguchi Y, Park JH, Inouye M. Toxin-antitoxin systems in bacteria and archaea. Annu Rev Genet 2011;45:61–79. doi: https://doi.org/10.1146/annurev-genet-110410-132412.
[10] Jurenaite M, Markuckas A, Suziedeliene E. Identification and characterization of type II toxin-antitoxin systems in the opportunistic pathogen *Acinetobacter baumannii*. J Bacteriol 2013;195(14):3165–72. doi: https://doi.org/10.1128/JB.00237-13.
[11] Awad LS, Abdallah DI, Mugharbil AM, Jisr TH, Droubi NS, El-Rajab NA, et al. Infectious Diseases Society of America/American Thoracic Society guidelines. Infect Drug Resist 2016;11(2018):17–28. doi: https://doi.org/10.2147/IDR.S145827.
[12] Huang Y, Zhou Q, Wang W, Huang Q, Liao J, Li J, et al. *Acinetobacter baumannii* ventilator-associated pneumonia: Clinical efficacy of combined antimicrobial therapy and in vitro drug sensitivity test results. Front Pharmacol 2019;10:92. doi: https://doi.org/10.3389/fphar.2019.00092.
[13] Dijkshoorn L, Nemec A, Seifert H. An increasing threat in hospitals: Multidrug-resistant *Acinetobacter baumannii*. Nat Rev Microbiol 2007;5(12):939–51. doi: https://doi.org/10.1038/nrmicro1789.
[14] Pendleton JN, Gorman SP, Gilmore BF. Clinical relevance of the ESKAPE pathogens. Expert Rev Anti Infect Ther 2013;11(3):297–308. doi: https://doi.org/10.1586/eri.13.12.

[15] Antunes LC, Visca P, Towner KJ. *Acinetobacter baumannii*: Evolution of a global pathogen. Pathog Dis 2014;71(3):292–301. doi: https://doi.org/10.1111/2049-632X.12125.
[16] Ciginskiene A, Dambrauskiene A, Rello J, Adukauskiene D. Ventilator-associated pneumonia due to drug-resistant *Acinetobacter baumannii*: Risk factors and mortality relation with resistance profiles, and independent predictors of in-hospital mortality. Medicina (Kaunas) 2019;55(2). doi: https://doi.org/10.3390/medicina55020049.
[17] Hong SH, Wang X, O'Connor HF, Benedik MJ, Wood TK. Bacterial persistence increases as environmental fitness decreases. Microb Biotechnol 2012;5 (4):509–22. doi: https://doi.org/10.1111/j.1751-7915.2011.00327.x.
[18] Harms A, Maisonneuve E, Gerdes K. Mechanisms of bacterial persistence during stress and antibiotic exposure. Science 2016;354(6318). doi: https://doi.org/10.1126/science.aaf4268.
[19] Fernandez-Garcia L, Fernandez-Cuenca F, Blasco L, Lopez-Rojas R, Ambroa A, Lopez M, et al. Relationship between tolerance and persistence mechanisms in *Acinetobacter baumannii* strains with AbkAB toxin-antitoxin system. Antimicrob Agents Chemother 2018;62(5). doi: https://doi.org/10.1128/AAC.00250-18.
[20] Woodall CA. Electroporation of E. coli. Methods Mol Biol 2003;235:55–69. doi: https://doi.org/10.1385/1-59259-409-3:55.
[21] Shao Y, Harrison EM, Bi D, Tai C, He X, Ou HY, et al. TADB: A web-based resource for type 2 toxin-antitoxin loci in bacteria and archaea. Nucleic Acids Res 2011;39(Database issue):D606–11. doi: https://doi.org/10.1093/nar/gkq908.
[22] Altschul SF, Gish W, Miller W, Myers EW, Lipman DJ. Basic local alignment search tool. J Mol Biol 1990;215(3):403–10. doi: https://doi.org/10.1016/S0022-2836(05)80360-2.
[23] Altschul SF, Madden TL, Schaffer AA, Zhang J, Zhang Z, Miller W, et al. Gapped BLAST and PSI-BLAST: A new generation of protein database search programs. Nucleic Acids Res 1997;25(17):3389–402. doi: https://doi.org/10.1093/nar/25.17.3389.
[24] Kumar S, Stecher G, Li M, Knyaz C, Tamura K. MEGA X: Molecular evolutionary genetics analysis across computing platforms. Mol Biol Evol 2018;35 (6):1547–9. doi: https://doi.org/10.1093/molbev/msy096.
[25] Aziz RK, Devoid S, Disz T, Edwards RA, Henry CS, Olsen GJ, et al. SEED servers: High-performance access to the SEED genomes, annotations, and metabolic models. PLoS ONE 2012;7(10):. doi: https://doi.org/10.1371/journal.pone.0048053e48053.
[26] Livak KJ, Schmittgen TD. Analysis of relative gene expression data using real-time quantitative PCR and the 2(-Delta Delta C(T)) Method. Methods 2001;25 (4):402–8. doi: https://doi.org/10.1006/meth.2001.1262.
[27] Zheng C, Xu J, Ren S, Li J, Xia M, Chen H, et al. Identification and characterization of the chromosomal *yefM-yoeB* toxin-antitoxin system of *Streptococcus suis*. Sci Rep 2015;5:13125. doi: https://doi.org/10.1038/srep13125.
[28] Piao H, Froula J, Du C, Kim TW, Hawley ER, Bauer S, et al. Identification of novel biomass-degrading enzymes from genomic dark matter: Populating genomic sequence space with functional annotation. Biotechnol Bioeng 2014;111 (8):1550–65. doi: https://doi.org/10.1002/bit.25250.
[29] Orth JD, Palsson BO. Systematizing the generation of missing metabolic knowledge. Biotechnol Bioeng 2010;107(3):403–12. doi: https://doi.org/10.1002/bit.22844.
[30] Aziz RK, Breitbart M, Edwards RA. Transposases are the most abundant, most ubiquitous genes in nature. Nucleic Acids Res 2010;38(13):4207–17. doi: https://doi.org/10.1093/nar/gkq140.
[31] Yamaguchi Y, Inouye M. Regulation of growth and death in *Escherichia coli* by toxin-antitoxin systems. Nat Rev Microbiol 2011;9(11):779–90. doi: https://doi.org/10.1038/nrmicro2651.
[32] Harms A, Brodersen DE, Mitarai N, Gerdes K. Toxins, targets, and triggers: An overview of toxin-antitoxin biology. Mol Cell 2018;70(5):768–84. doi: https://doi.org/10.1016/j.molcel.2018.01.003.
[33] Howard A, O'Donoghue M, Feeney A, Sleator RD. *Acinetobacter baumannii*: An emerging opportunistic pathogen. Virulence 2012;3(3):243–50. doi: https://doi.org/10.4161/viru.19700.
[34] Brown JM, Shaw KJ. A novel family of *Escherichia coli* toxin-antitoxin gene pairs. J Bacteriol 2003;185(22):6600–8. doi: https://doi.org/10.1128/jb.185.22.6600-6608.2003.
[35] Wen Z, Wang P, Sun C, Guo Y, Wang X. Interaction of type IV toxin/antitoxin Systems in cryptic prophages of *Escherichia coli* K-12. Toxins (Basel) 2017;9(3). doi: https://doi.org/10.3390/toxins9030077.
[36] Sat B, Hazan R, Fisher T, Khaner H, Glaser G, Engelberg-Kulka H. Programmed cell death in *Escherichia coli*: Some antibiotics can trigger *mazEF* lethality. J Bacteriol 2001;183(6):2041–5. doi: https://doi.org/10.1128/JB.183.6.2041-2045.2001.
[37] Juttukonda LJ, Green ER, Lonergan ZR, Heffern MC, Chang CJ, Skaar EP. *Acinetobacter baumannii* OxyR regulates the transcriptional response to hydrogen peroxide. Infect Immun 2019;87(1). doi: https://doi.org/10.1128/IAI.00413-18.
[38] Narimisa N, Amraei F, Kalani BS, Mohammadzadeh R, Jazi FM. Effects of sub-inhibitory concentrations of antibiotics and oxidative stress on the expression of type II toxin-antitoxin system genes in *Klebsiella pneumoniae*. J Glob Antimicrob Resist 2020;21:51–6. doi: https://doi.org/10.1016/j.jgar.2019.09.005.
[39] Jensen RB, Gerdes K. Programmed cell death in bacteria: Proteic plasmid stabilization systems. Mol Microbiol 1995;17(2):205–10. doi: https://doi.org/10.1111/j.1365-2958.1995.mmi_17020205.x.
[40] Van Melderen L, Saavedra De Bast M. Bacterial toxin-antitoxin systems: More than selfish entities?. PLoS Genet 2009;5(3):. doi: https://doi.org/10.1371/journal.pgen.1000437e1000437.
[41] Guzman LM, Belin D, Carson MJ, Beckwith J. Tight regulation, modulation, and high-level expression by vectors containing the arabinose PBAD promoter. J Bacteriol 1995;177(14):4121–30. doi: https://doi.org/10.1128/jb.177.14.4121-4130.1995.